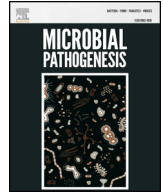




Since January 2020 Elsevier has created a COVID-19 resource centre with free information in English and Mandarin on the novel coronavirus COVID-19. The COVID-19 resource centre is hosted on Elsevier Connect, the company's public news and information website.

Elsevier hereby grants permission to make all its COVID-19-related research that is available on the COVID-19 resource centre - including this research content - immediately available in PubMed Central and other publicly funded repositories, such as the WHO COVID database with rights for unrestricted research re-use and analyses in any form or by any means with acknowledgement of the original source. These permissions are granted for free by Elsevier for as long as the COVID-19 resource centre remains active.



# Isolation and characterization of a variant subgroup GII-a porcine epidemic diarrhea virus strain in China

Dan Yang<sup>a,1</sup>, Mingjun Su<sup>a,1</sup>, Chunqiu Li<sup>a</sup>, Bei Zhang<sup>a</sup>, Shanshan Qi<sup>a</sup>, Dongbo Sun<sup>a,b,\*</sup>,  
Baishuang Yin<sup>b,\*\*</sup>

<sup>a</sup> Laboratory for the Prevention and Control of Swine Infectious Diseases, College of Animal Science and Veterinary Medicine, Heilongjiang Bayi Agricultural University, Daqing, China

<sup>b</sup> College of Animal Science and Technology, Jilin Agricultural Science and Technology University, Jilin, China

## ARTICLE INFO

### Keywords:

Porcine epidemic diarrhea virus  
Variant strain  
Pathogenicity  
Vaccine

## ABSTRACT

**Background:** Highly virulent variants of porcine epidemic diarrhea virus (PEDV) have been closely associated with recent outbreaks of porcine epidemic diarrhea (PED) in China, which have resulted in severe economic losses to the pork industry.

**Methods:** In the current study, the variant PEDV strain HM2017 was isolated and purified and a viral growth curve was constructed according to the median tissue culture infective dose (TCID<sub>50</sub>). HM2017 were amplified with RT-PCR and analyzed by phylogeny analysis. Animal pathogenicity experiment was carried out to evaluate the HM2017 clinical assessment.

**Results:** Genome-based phylogenetic analysis revealed that PEDV strain HM2017 was clustered into the variant subgroup GII-a that is currently circulating in pig populations in China. The highest median tissue culture infectious dose of strain HM2017 after 15 passages in Vero cells was  $1.33 \times 10^7$  viral particles/mL. Strain HM2017 was highly virulent to suckling piglets, which exhibited clinical symptoms at 12 h post-infection (hpi) (i.e., weight loss at 12–84 hpi, increased body temperatures at 24–48 hpi, high viral loads in the jejunum and ileum, and 100% mortality by 84 hpi).

**Conclusion:** The present study reports a variant subgroup GII-a PEDV HM2017 strain in China and characterizes its pathogenicity. PEDV strain HM2017 of subgroup GII-a presents a promising vaccine candidate for the control of PED outbreaks in China.

## 1. Introduction

Porcine epidemic diarrhea virus (PEDV) is an enveloped, single-stranded, positive-sense RNA virus belonging to the genus *Alphacoronavirus*. In 1978, PEDV was identified as the causative agent of porcine epidemic diarrhea (PED) [1], which is characterized by acute watery diarrhea, vomiting, and dehydration, with high mortality often reaching 100% in neonatal piglets. At the end of 2010, a PEDV outbreak occurred in several pig-producing provinces in southern China [2,3]. Since then, the disease has spread throughout other provinces, which has resulted in enormous economic losses to the pork industry in China [4,5]. At present, PEDV infection is widely circulated in swine-farming countries in Asia, Europe, and North America [6–9]. The emergence

and re-emergence of PEDV have resulted in severe economic losses and poses significant public health concerns worldwide.

Point, insertion, and deletion mutations of the PEDV genome have been frequently reported, leading to the genetic diversities of PEDV epidemic strains [10–12]. According to the nucleotide sequences of the viral complete genome, PEDV strains are classified into the classic GI group or the variant GII group [13,14]. The GI group includes the subgroups GI-a and GI-b, while the GII group consists of the subgroups GII-a and GII-b. Global PEDV strains are also defined as the S-INDEL and non-S-INDEL strains, which correspond to the GI and GII groups, respectively, according to mutations of the spike (S) protein of PEDV [10,15,16]. In China, the variant subgroups GII-a and GII-b are classified as PEDV pandemic strains circulating in pig populations

\* Corresponding author. Laboratory for the Prevention and Control of Swine Infectious Diseases, College of Animal Science and Veterinary Medicine, Heilongjiang Bayi Agricultural University, Daqing, China.

\*\* Corresponding author.

E-mail addresses: [dongbosun@126.com](mailto:dongbosun@126.com) (D. Sun), [ybs3421@126.com](mailto:ybs3421@126.com) (B. Yin).

<sup>1</sup> These authors contributed equally to this work.

[9,14,17,18]. Recently, Guo et al. (2019) analyzed the complete genomes of 409 PEDV strains from different countries, which were classified into five subgroups strains (GI-a, GI-b, GII-a, GII-b, and GII-c) [14]. Recombination analysis indicated that the GII-c subgroup strains evolved from a recombination event between subgroups GI-a and GII-a. These data suggest that the Chinese PEDV pandemic strains have undergone genetic variations, leading to the genetic diversities of PEDV pandemic strains.

The genotypes of PEDV are closely associated with pathogenicity and immune protection [16,19–21]. The PEDV subgroups GII-a and GII-b in China are highly pathogenic to sucking piglets and exhibit serum cross-neutralization activity or cross-immune protection. The GII-a subgroup of PEDV was found to mediate better immune protection against challenges with the homologous PEDV strain than with the GII-b subgroup strain [5,18,22,23]. The objective of the current study was to reveal the molecular characteristics of the isolated subgroup GII-a PEDV strain HM2017, and evaluate its molecular characteristics and pathogenesis.

## 2. Methods

### 2.1. Viral isolation and identification

PEDV-positive intestinal tissues samples collected in China from 2015 to 2018 were chosen for viral isolation. Identification of the PEDV-positive samples was performed according to the methods described by Wang et al. (2016) [12]. Viral isolation was conducted in accordance with the PEDV isolation protocol described by Jiang et al. (2018) [24]. Upon the development of a cytopathic effect (CPE), the viruses were harvested from the culture supernatant for serial passages. The isolated viruses were identified by electron microscopy (EM) and with the use of an indirect immunofluorescence assay (IFA). For the IFA, Vero cells were inoculated with PEDV isolates at a multiplicity of infection of 0.1 for 36 h and then were fixed with paraformaldehyde (4%). After blocking with 5% skim milk for 2 h at room temperature, the cells were incubated with primary monoclonal antibodies (dilution,  $\times 500$ ) against the spike (S) protein of PEDV for 1 h at 37 °C followed by fluorescein isothiocyanate-conjugated donkey anti-mouse antibody against immunoglobulin G (dilution,  $\times 2000$ ; Thermo Fisher Scientific, Waltham, MA, USA). The monoclonal antibodies against the spike (S) protein was kindly provided by the Division of Swine Digestive System Infectious Diseases, State Key Laboratory of Veterinary Biotechnology, Harbin Veterinary Research Institute, Chinese Academy of Agricultural Sciences. The cells were then observed under a fluorescence microscope. For EM, the samples were negatively stained as previously described (Jiang et al., 2018). The viral suspension was subjected to ultracentrifugation at  $30,000 \times g$  for 30 min to pellet the viral particles, which were negatively stained with 2% phosphotungstic acid (pH 7.0). The negatively stained samples were examined using a Hitachi-7650 transmission electron microscope (Hitachi, Ltd., Tokyo, Japan). The PEDV isolate was named strain HM2017.

### 2.2. Virus purification and growth curve

PEDV strain HM2017 was purified by plaque cloning in Vero cells. Briefly, Vero cells were incubated with serially diluted PEDV strain HM2017 in post-inoculation medium at 37 °C for 2 h under an atmosphere of 5% CO<sub>2</sub>. Afterward, the medium was removed and the cells in each well were overlaid with 2 mL of post-inoculation medium containing 1.5% agarose. After the overlaid medium had solidified, the cells were grown at 37 °C under an atmosphere of 5% CO<sub>2</sub> to promote plaque formation. Macroscopically visible plaques were picked with a pipette pick, dissolved in 1 mL of DMEM, frozen and thawed for three times after receiving poison, and then inoculated in Vero cells for propagation in preparation for the next round of plaque purification. The plaque purification operation was repeated five times. After

incubation for 48 h, the agarose was covered. When plaques grew to the proper size, the cells were fixed in paraformaldehyde (4%) for 2 h and the plaques were visualized by staining with crystal violet.

Viral growth curves of PEDV strains HM2017 in Vero cells was constructed according to the median tissue culture infective dose (TCID<sub>50</sub>). Briefly, Vero cells were seeded in the wells of 96-well plates at a density of  $10^5$  cells per well in 100  $\mu$ L of medium and incubated for 48 h at 37 °C under an atmosphere of 5% CO<sub>2</sub>. Afterward, the medium was removed and 100  $\mu$ L of 10-fold serial dilutions of the virus were added to each well. The cytopathic effect was examined every 12 h for 5 days post-inoculation. The viral titer was determined according to the Reed and Muench method [25]. The classic PEDV strain CV777 was used as a control. PEDV strain CV777 (GenBank accession no. [KT323979](https://www.ncbi.nlm.nih.gov/nuclot/KT323979); group I) was kindly provided by the Division of Swine Digestive System Infectious Diseases, State Key Laboratory of Veterinary Biotechnology, Harbin Veterinary Research Institute, Chinese Academy of Agricultural Sciences.

### 2.3. Genome sequencing and phylogeny analysis

A total of 30 pairs of primers were designed to amplify the complete genome of PEDV strain HM2017 by conventional reverse transcription polymerase chain reaction (RT-PCR) (Table S1). Briefly, RNA extraction and cDNA synthesis were performed in accordance with the protocols described by Wang et al. (2016) [12]. The RT-PCR amplification protocol included an initial denaturation step at 98 °C for 30 s, followed by 30 cycles at 98 °C for 10 s, 55 °C for 30 s, 72 °C for 90 s, and a final extension at 72 °C for 10 min. After purification, the RT-PCR products of each gene fragment were sequenced three times. The complete genome of PEDV strain HM2017 (GenBank accession no. [MK690502](https://www.ncbi.nlm.nih.gov/nuclot/MK690502)) was assembled according to the sequencing results of 30 gene fragments and the nucleotide sequences were submitted to the GenBank database (<https://www.ncbi.nlm.nih.gov/genbank/>).

For genotyping of PEDV strain HM2017, the entire genomes and S genes of 532 PEDV strains from different geographical locations within China and the rest of the world were retrieved from the NCBI nucleotide database as reference sequences, which included the subgroups GI-a, GI-b, GII-a, GII-b, and GII-c. The genomic sequences of the PEDV reference strains were used to generate a neighbor-joining phylogenetic tree with the use of the ClustalX alignment tool of the MEGA6.06 software package [26]. Neighbor-joining phylogenetic trees were constructed with the p-distance model, 1000 bootstrap replicates, and otherwise default parameters using MEGA 6.06 software. The phylogenetic trees were pruned and re-rooted using Interactive Tree Of Life software version 4.2.3 (<https://itol.embl.de/>), which is an online tool for displaying of circular trees and annotations [27]. In addition, similarity plots of the genomes of the PEDV strains identified in the present study was created using the sliding window method as implemented in the SimPlot, v.3.5.1 package [28].

### 2.4. Animal experimental design

The protocols of the animal experiments were approved by the Animal Experiment Ethical Committee of Heilongjiang Bayi Agricultural University (approval no. 201501003; Daqing, Heilongjiang province, China). Twenty-four newborn piglets were selected and confirmed to be negative for PEDV, transmissible gastroenteritis virus, and porcine rotavirus with the Colloidal gold rapid detection kit (BioNote, Hwaseong-si, Gyeonggi-do, Republic of Korea). Then, the piglets were randomly assigned to one of two groups, i.e., the PEDV HM2017 inoculation group (n = 18) or the control group (n = 6), which were housed in separate cages. Piglets in the inoculation group were orally inoculated with 3 mL of Dulbecco's modified Eagle's medium (DMEM) containing  $1.33 \times 10^6$  TCID<sub>50</sub> of PEDV strain HM2017, while the control group was orally administered 3 mL of virus-free DMEM.

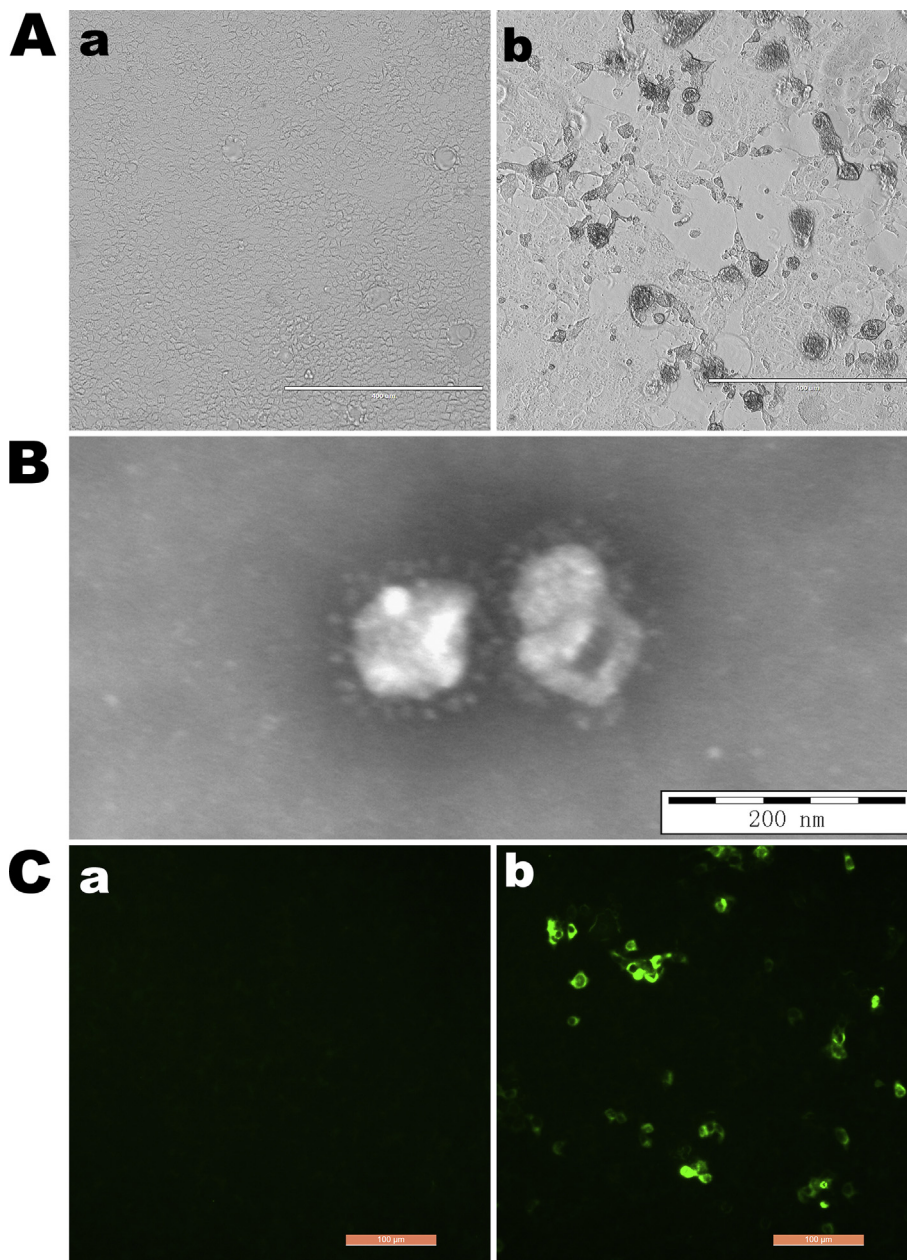


**Fig. 1.** Identification of the isolated PEDV HM2017 strain (P8). (A) Cytopathic effects of the PEDV HM2017 strain on Vero cells at 36 h post-inoculation (hpi) (100 $\times$  magnification). (a) Mock-inoculated Vero cells culture showing normal cells. (b) HM2017-inoculated Vero cells showing rounded and clustered cells. (B) Electron microscopy of the supernatants of the HM2017-inoculated Vero cells by using negative staining with phosphotungstic acid. Typical coronavirus-like particles were visible (Scale bar = 200 nm). (C) Detection of PEDV HM2017 strain in Vero cells by immunofluorescence (IF) staining using *monoclonal antibody against spike protein of PEDV* at 36 hpi (200 $\times$  magnification). (a) IF staining of mock-inoculated Vero cells showing no IF-positive cells. (b) IF-stained cells were visible in HM2017-inoculated Vero cells.

Fecal swabs were collected before inoculation and then every 12 h until death. Six piglets from the inoculated group and three from the control group were necropsied at 36 h post-infection (hpi). At necropsy, tissue samples of the heart, liver, spleen, lung, kidney, stomach, duodenum, jejunum, ileum, cecum, and colon were collected and then formalin-fixed. Fresh tissue samples were stored at  $-80^{\circ}\text{C}$  for viral RNA distribution analysis and formalin-fixed samples were used for histological and immunohistochemical analyses.

### 2.5. Clinical assessment

The piglet body temperatures and weights were recorded before inoculation ( $-12$  hpi) and then every 12 h until death. All piglets were evaluated twice daily for clinical signs of lethargy and diarrhea [29]. The clinical mental state of all piglets was scored according to the following criteria: 0 = normal; 1 = mild lethargy (slow to move, head down); 2 = moderate lethargy (able to stand, but tended to lie down); 3 = heavier lethargy (tended to lie down, but occasionally stood); 4 = severe lethargy (recumbent, moribund). Diarrhea severity was

scored according to the following criteria: 0 = normal; 1 = soft (“cow pies”); 2 = very soft and tended to be liquid; 3 = liquid with some solid content; 4 = watery diarrhea with no solid content. In addition, the mortality of the piglets in each group was recorded twice daily.

### 2.6. Virus shedding and distribution

Each fecal swab was diluted and homogenized in 1 mL of sterile  $1 \times$  phosphate-buffered saline (pH 7.4) and then centrifuged at  $4200 \times g$  at  $4^{\circ}\text{C}$  for 10 min. The supernatant was collected for viral RNA extraction. Equal quantities (1 g) of tissue samples were homogenized in 5 mL of DMEM. After centrifugation at  $4200 \times g$  at  $4^{\circ}\text{C}$  for 10 min, the supernatant was used for RNA extraction and subsequent cDNA synthesis, which were performed according to the protocols described by Wang et al. (2016) [12]. PEDV cDNA was generated by RT-qPCR with primers targeting the ORF3 gene (sense: 5'-GAC AAG CTT CAA ATG TGA CGG G-3'; antisense: 5'-AAT GAC AGC AAA ACG CGC TG-3'). Standard plasmids were constructed for use in the present study. Briefly, the entire ORF3 gene of PEDV strain HM2017 was amplified

using specific primers as described by Wang et al. (2016) [12] and the RT-qPCR products were cloned into the pMD18-T plasmid (Takara Bio, Inc., Otsu, Shiga, Japan). RT-qPCR was performed using SYBR Green I fluorescent dye and a QuantStudio™ 3 Real-Time PCR System (Applied Biosystems, Carlsbad, CA, USA). For RT-qPCR, each 20- $\mu$ L reaction system included 10  $\mu$ L of 2  $\times$  SYBR® Premix Ex Taq polymerase (Takara Bio, Inc.), 2  $\mu$ L of cDNA, and 0.25  $\mu$ M of each primer. Reaction conditions were set as follows: denaturation at 95 °C for 30 s, followed by 40 cycles at 95 °C for 25 s and 60 °C for 60 s. In each plate, 10-fold dilutions of the standard plasmid (from 10<sup>10</sup> to 10<sup>0</sup>) and the negative control (distilled water) were included. Each sample was assayed three times. The quantity of PEDV viral RNA was calculated based on the results of the standard plasmid.

## 2.7. Histological and immunohistochemical analyses

Histological and immunohistochemical analyses were performed in accordance with the procedures described by Dong et al. (2016) [30]. At necropsy, tissue samples of the duodenum, jejunum, ileum, cecum, and colon of the piglets from the inoculated and control groups were collected separately. After fixation for 36 h in 10% formalin at room temperature, the tissue specimens were processed and embedded in paraffin. The paraffin-embedded tissues were cut into 5  $\mu$ m-thick sections using a microtome (Zhejiang Jinhua Kedi Instrumental Equipment Co., Ltd. Jinhua, Zhejiang province, China). The sections were then deparaffinized with xylene, washed in decreasing concentrations of ethanol, and stained with hematoxylin and eosin (Beijing Solarbio Science & Technology Co., Ltd., Beijing, China) for histopathological analysis or subjected to immunohistochemical staining using PEDV-specific mouse antisera (dilution, 1:200) (prepared in our laboratory).

## 2.8. Statistical analysis

All statistical analyses were conducted using GraphPad Prism 8.0 software (GraphPad Software, Inc., La Jolla, CA, USA) and significance was assessed using the Student's *t*-test. Probability (*p*) values of < 0.05 and < 0.01 were considered statistically significant and highly significant, respectively.

## 3. Results

### 3.1. Viral isolation and identification

Of the PEDV-positive samples, one sample (HM2017) from Mudanjiang city in Heilongjiang province showed a remarkable cytopathic effect in Vero cells at the beginning of passage 8 (P8) when compared with the control cells (Fig. 1A). Positive results for PEDV strain HM2017 (P8) were confirmed with the use of RT-PCR targeting the ORF3 gene (data not shown) and IFA based on a monoclonal antibody against the S protein of PEDV (Fig. 1B). EM confirmed the presence of typical coronavirus-like particles in the suspensions of strain HM2017 (P8)-infected Vero cells, which had diameters of about 150 nm (Fig. 1C). PEDV strain HM2017 (P8) was successfully purified by plaque cloning in Vero cells and the purified viruses were serially passaged for 15 generations in Vero cells (Fig. 2A). After verification of generation 15 of PEDV strain HM2017 by RT-PCR, EM, and IFA, according to the above-mentioned methods (data not shown), a growth curve was generated based on the TCID<sub>50</sub> values. The results indicated that the proliferative ability of PEDV strain HM2017 (P15) in Vero cells was significantly higher than that of the classical strain CV777, as the titer of strain HM2017 (P15) reached 3.83  $\times$  10<sup>4</sup>, 6.81  $\times$  10<sup>5</sup>, 4.47  $\times$  10<sup>6</sup>, 7.50  $\times$  10<sup>6</sup>, 1.33  $\times$  10<sup>7</sup>, 1.10  $\times$  10<sup>7</sup> TCID<sub>50</sub>/mL in Vero cells at 12, 24, 36, 48, 60, and 72 hpi, respectively (Fig. 2B).

### 3.2. Phylogenetic analysis of PEDV strain HM2017

The complete genomic sequence of PEDV strain HM2017 (P15) was successfully obtained and deposited to the GenBank database under the accession no. MK690502. The genome of strain HM2017 is composed of 28,035 nucleotides. Sequence comparisons of the whole genomes revealed nucleotide homologies of 96.1%–99.7% between strain HM2017 and 532 PEDV reference strains (GI-a, GI-b, GII-a, GII-b, and GII-c). The genome-based phylogenetic tree showed that the 533 PEDV strains were classified into two groups: group I (GI: classical strains) and group II (GII: variant strains). Group II was composed of three subgroups GII-a, GII-b, and GII-c (Fig. 3A). The PEDV strain HM2017, which was identified in the present study, was clustered into the subgroup GII-a, which consists of the strain HM2017 and 384 PEDV reference strains from China during 2011–2018. The PEDV strains of the subgroup GII-a formed different clades, exhibiting genetic diversities. The S gene was 4158 nucleotides in length, encoding a protein of 1386 amino acids (aa). Sequence analysis of the S protein of HM2017 strain showed that compared with PEDV strain CV777, two insertion were found at positions 58–59 (a 4-aa insertion of QGVN) and 135–136 (a 1-aa insertion of N), and a 2-aa deletion (DI) and 1-aa deletion (Y) were found at positions 158–159 and 1194 (amino acids are numbered according to the S protein of the PEDV strain CV777). Phylogenetic analysis based on the S gene indicated that the HM2017 strain belonged to subgroup GIIa (Fig. 3B). Genomic similarity analysis revealed that PEDV strain HM2017 exhibited divergence from the reference strains of group GI and subgroup GII-c at part of the S1 gene. The PEDV strain HM2017 exhibited high similarity with reference strains from the subgroups GII-a and GII-b (Fig. 4).

### 3.3. Pathogenicity of PEDV strain HM2017

In the present study, the pathogenicity results of GII-a subgroup PEDV strain HM2017 in suckling piglets are shown in Figs. 5 and 6. Of the 18 piglets in the experimental group, 12 (66.67%) exhibited mild diarrhea at 12 hpi and all 18 showed mild diarrhea and vomiting at 24 hpi. At 36 hpi, all piglets (18/18, 100%) in the experimental group developed severe watery diarrhea, vomiting, and dehydration, and then died by 84 hpi. Notably, the piglets in the experimental group had significantly higher body temperatures at 36 hpi (*p* < 0.05) and exhibited gradual weight loss, as compared to those in the control group.

Viral shedding was evaluated in all experimental piglets with the use of rectal swab samples that were subjected to RT-qPCR targeting the PEDV ORF3 gene. Viral distribution in tissues was detected and analyzed with the use of RT-qPCR targeting the PEDV ORF3 gene. The results indicated that all piglets in the control group were negative for PEDV, while those in the experimental group exhibited high levels (4.57  $\times$  10<sup>7</sup> to 2.06  $\times$  10<sup>8</sup> RNA copies/mL) of virus shed in feces from 12 to 84 hpi (Fig. 7A). High levels of viral RNA were identified in the duodenum (4.69  $\times$  10<sup>5</sup> RNA copies/g), jejunum (7.75  $\times$  10<sup>7</sup> RNA copies/g), ileum (9.33  $\times$  10<sup>7</sup> RNA copies/g), cecum (2.06  $\times$  10<sup>6</sup> RNA copies/g), and colon (3.06  $\times$  10<sup>7</sup> RNA copies/g) at 36 hpi. Also, viral loads were greater in the jejunum and ileum than in other intestinal tissues (Fig. 7B). At necropsy, gross lesions were found throughout the gastrointestinal tract. The clinical manifestations of PEDV infection of the stomach were distension due to undigested milk curd, while the small intestinal tract was distended, transparent, and filled with yellow fluid (Fig. 8A). Histopathological analysis indicated shortening, fusion, and sloughing of the small intestinal villi of the PEDV-infected piglets (Fig. 8B). Immunohistochemical analysis showed that PEDV virions were present in the cytoplasm of the epithelial cells of the atrophied small intestinal villi of the PEDV-infected piglets (Fig. 8C).

## 4. Discussion

The Chinese PEDV epidemic strains exhibited genetic diversity due

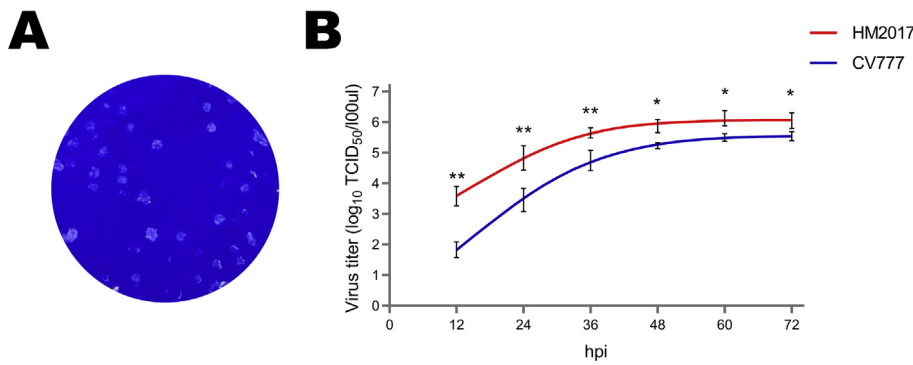


Fig. 2. Plaque purification and viral growth kinetic of PEDV HM2017 strain (P15). (A) Plaque purification of PEDV HM2017 strain. Monolayers of Vero cells were inoculated with PEDV HM2017 strain. After incubation for 2 h, the cells overlaid with 1.5% agarose. Plaques were stained with crystal violet at 48 hpi. (B) Viral growth kinetics in Vero cells. Vero cells were inoculated with PEDV HM2017 strain and PEDV CV777 strain at MOI = 0.01, respectively. Virus titers at different time points were determined and the 50% tissue culture infectious dose (TCID<sub>50</sub>) was calculated. Asterisk (\*) indicates a significant difference between PEDV HM2017 strain and PEDV CV777 strain (\*,  $P < 0.05$ ; \*\*,  $P < 0.01$ ).

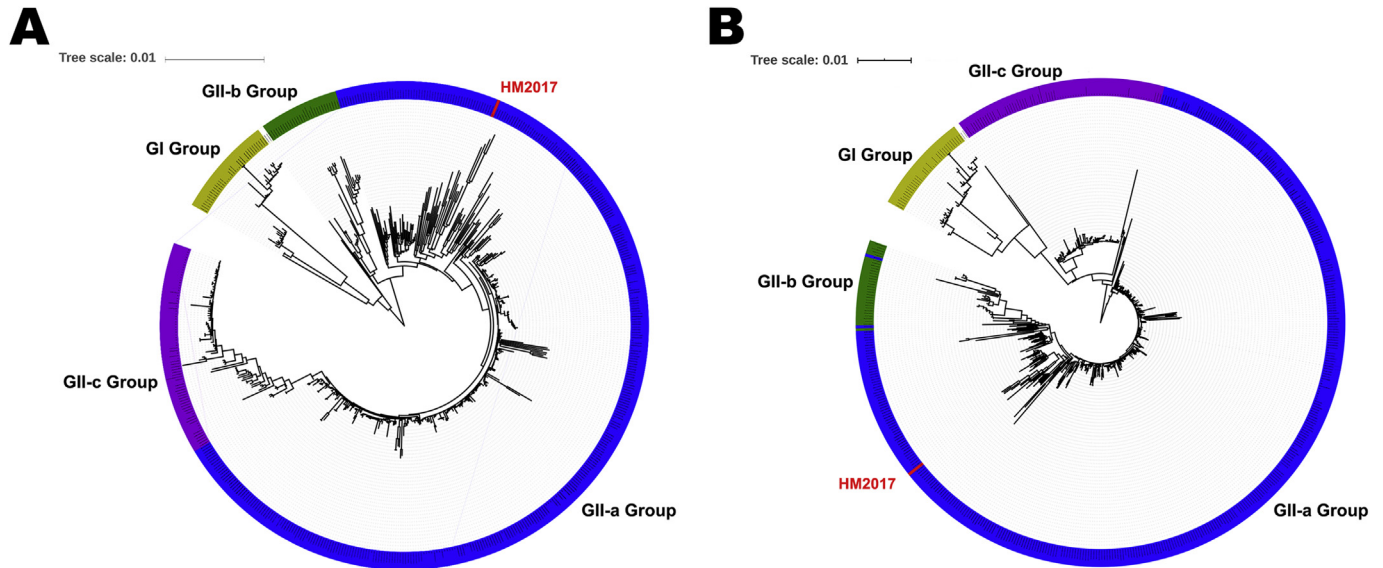


Fig. 3. (A) Phylogenetic analysis based on the complete genome nucleotide sequence of PEDV HM2017 strain and 532 reference PEDV strains. (B) Phylogenetic analysis based on the S gene nucleotide sequence of PEDV HM2017 strain and 532 reference PEDV strains. PEDV HM2017 strain is indicated with a red triangle. The phylogenetic tree was constructed with the neighbor-joining method with 1000 bootstrap replications using MEGA 6.06 software.

to immune pressures and the high mutation rate of the RNA genome, and formed various subgroups or clusters. The various epidemic strains of PEDV differ in virulence and immunity, leading to incomplete immune protection of commercial vaccines against infection with various

PEDV epidemic strains. In order to investigate the genetic evolution and pathogenic characteristics of PEDV, viral isolation was conducted using PEDV-positive samples collected in China from 2015 to 2018. In the present study, the PEDV strain HM2017 was successfully isolated from

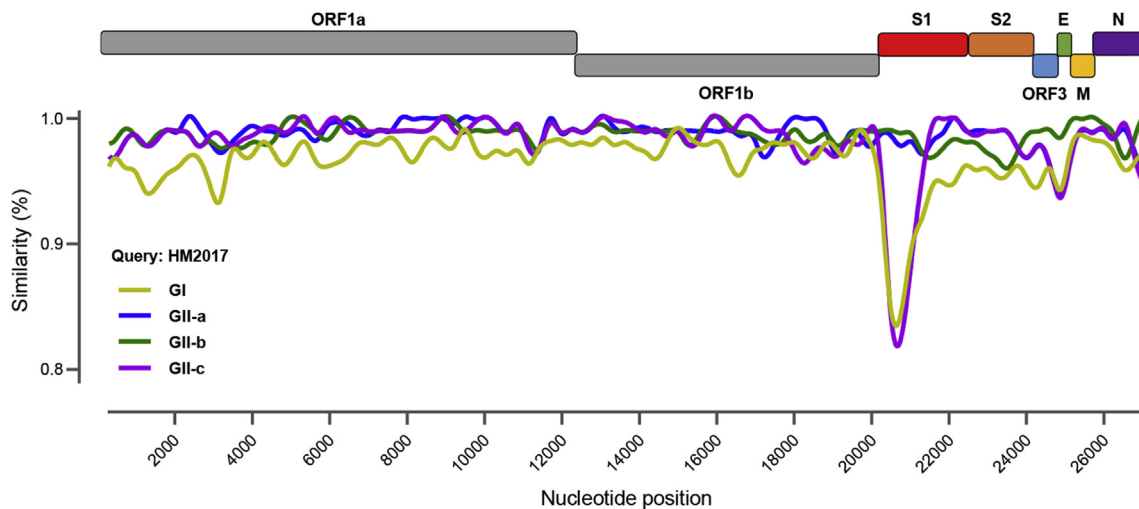


Fig. 4. Similarity plot of the complete genome nucleotide sequence of PEDV HM2017 strain and 532 reference PEDV strains. Note. PEDV HM2017 strain was set as query strain; the vertical and horizontal axes indicated the nucleotide similarity percent and nucleotide position (bp) in the graph, respectively.

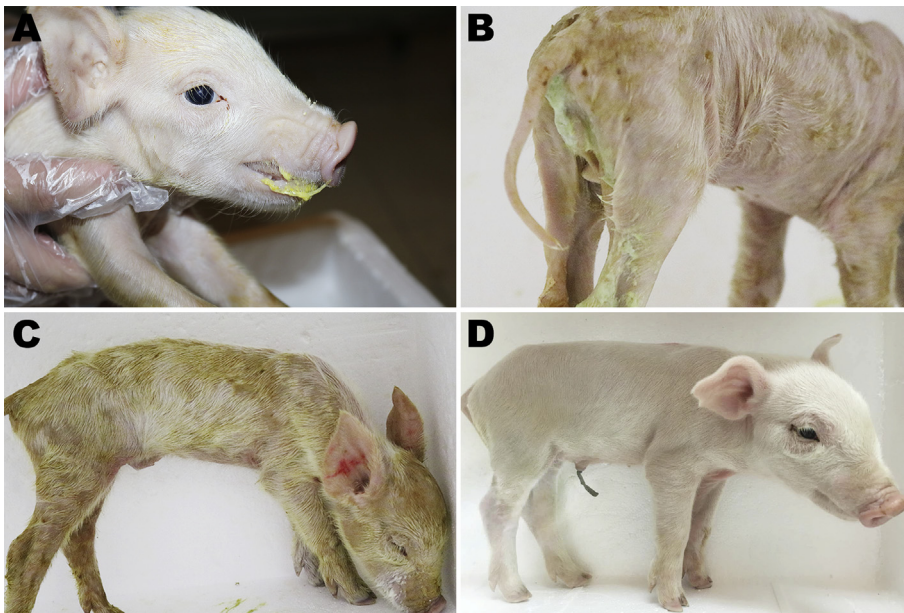


Fig. 5. Clinical assessment of piglets challenged with PEDV HM2017 strain. (A) Vomiting and (B) watery diarrhea were observed at 24 hpi with PEDV HM2017 strain. (C) Severe lethargy (recumbent, moribund) was observed at 72 hpi with PEDV HM2017 strain. (D) The piglets inoculated with control medium showing no clinical symptoms.

Vero cells and showed good cellular adaptability, as the viral titer of passage 15 was  $1.33 \times 10^7$  TCID<sub>50</sub>/mL. The PEDV strain HM2017 was classified to the variant subgroup GII-a. Moreover, PEDV strain HM2017 was strongly virulent to suckling piglets, as characterized by severe clinical symptoms, high viral RNA titers shed in feces, gross lesions within the small intestine, shortening of the small intestinal villi, and a mortality rate of 100% by 84 hpi.

The global PEDV strains are classified into the classic GI group and variant GII group [4,6]. The PEDV strains in the variant GII group are

closely related to the frequent occurrence of porcine epidemic diarrhea, which has resulted in huge economic losses to the pork industry worldwide [9,13]. The PEDV strains in the variant GII group appear to be genetically diverse with a gradual increase in number reported globally. Guo et al. (2019) reported that group GII PEDV strains can be classified into subgroups GII-a, GII-b, and GII-c, according to phylogenetic analysis of 409 complete genomes of global strains, of which the GII-c is a newly discovered subgroup [14]. In fact, the GII-c subgroup was genetically separated from the GII-a subgroup due to the

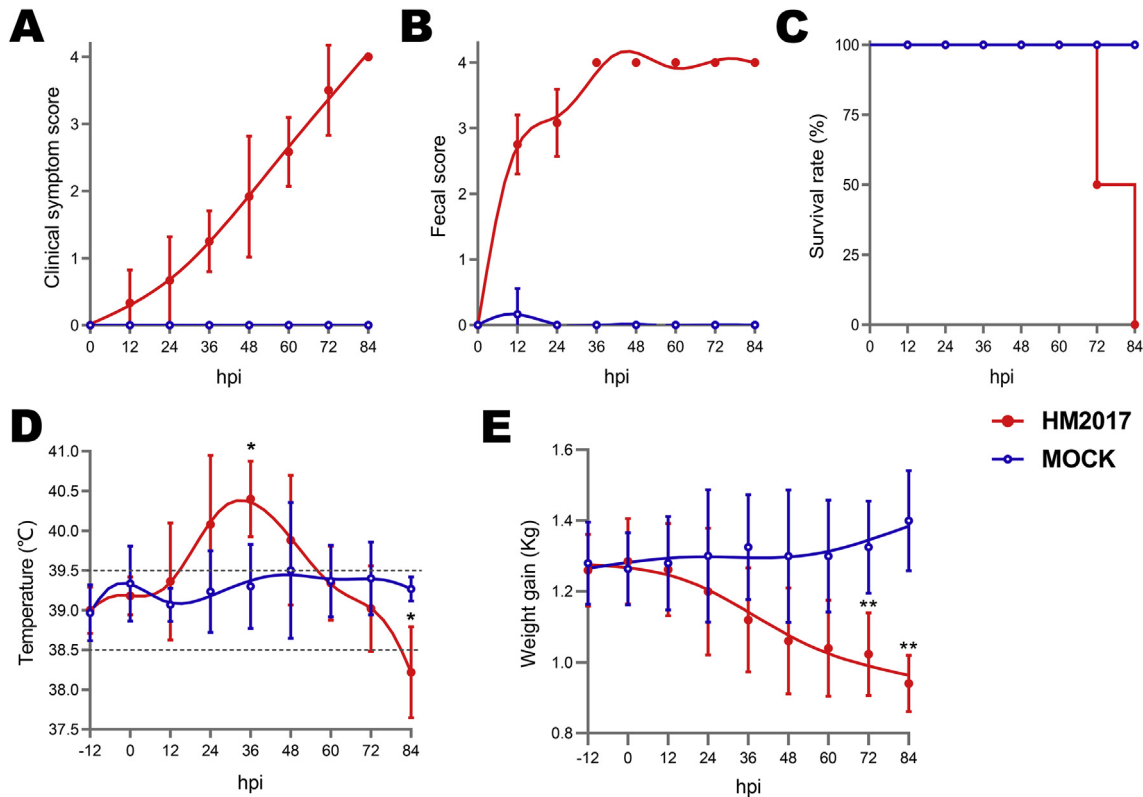
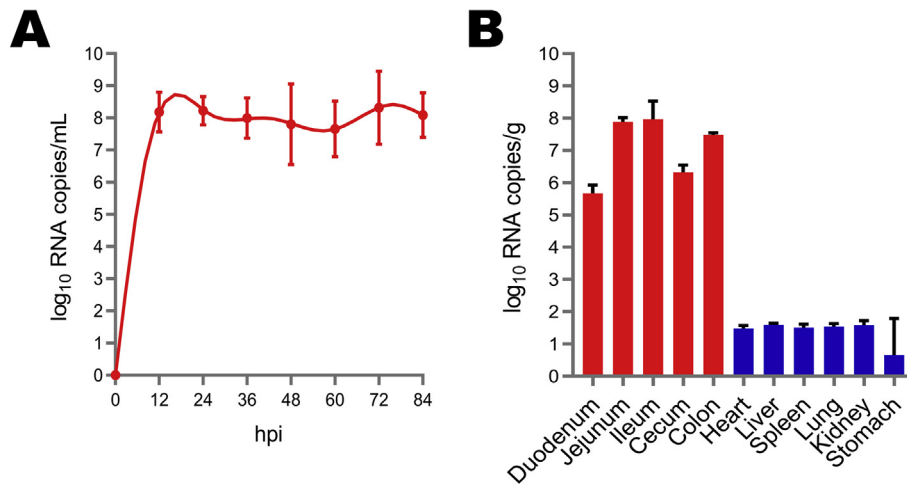


Fig. 6. Pathogenicity analysis of PEDV HM2017 strain. (A) The clinical symptom scores of piglets in each group. (B) The fecal scores of piglets in each group. (C) The survival rate of piglets in each group. (D) The average body temperature of piglets in each group. (E) The average body weight changes of piglets in each group. Asterisk (\*) indicates a significant difference between HM2017-inoculated group and control group (\*,  $P < 0.05$ ; \*\*,  $P < 0.01$ ).



**Fig. 7.** Fecal viral shedding and virus distribution in PEDV HM2017-inoculated piglets. (A) Virus shedding in rectal swabs in HM2017-inoculated piglets. (B) Virus distribution at 36 hpi in HM2017-inoculated piglets.

inconsistent topologies between the S gene and other genes. In the present study, a genome-based phylogenetic tree of 532 global PEDV reference strains was generated. These PEDV reference strains included subgroups GI-a, GI-b, GII-a, GII-b, and GII-c (the genotype of each has been defined in previous studies). In the present study, PEDV strain HM2017 and 384 Chinese PEDV reference strains formed the group GII-a, and the PEDV strains from the subgroup GII-a showed genetic diversities. The results of genomic similarity analysis indicated that the PEDV strain HM2017 exhibited high similarity with these reference strains from the subgroups GII-a and GII-b. The PEDV HM2017 strain identified in our study and seven reference strains formed a unique clade, differing genetically from other reference strains of the subgroup

GII-a. These data suggest that Chinese PEDV subgroups GII-a strains have undergone genetic variations, forming potential novel clades.

The pathogenicity of different PEDV subgroups has been widely investigated and many reports have confirmed that the PEDV strains of the subgroups GII-a and GII-b are highly pathogenic to suckling piglets, with infection manifesting as severe clinical symptoms with watery diarrhea, vomiting, and dehydration, high viral loads shed in the stool, severe lesions within the intestine, as evidenced by thin-transparent intestinal walls and intestinal villus atrophy or shedding, loss of bodyweight, and rapid death [19,20,29,31,32]. In the present study, PEDV strain HM2017 of subgroup GII-a was strongly virulent to suckling piglets, similar to that of the PEDV strains of subgroups GII-a and

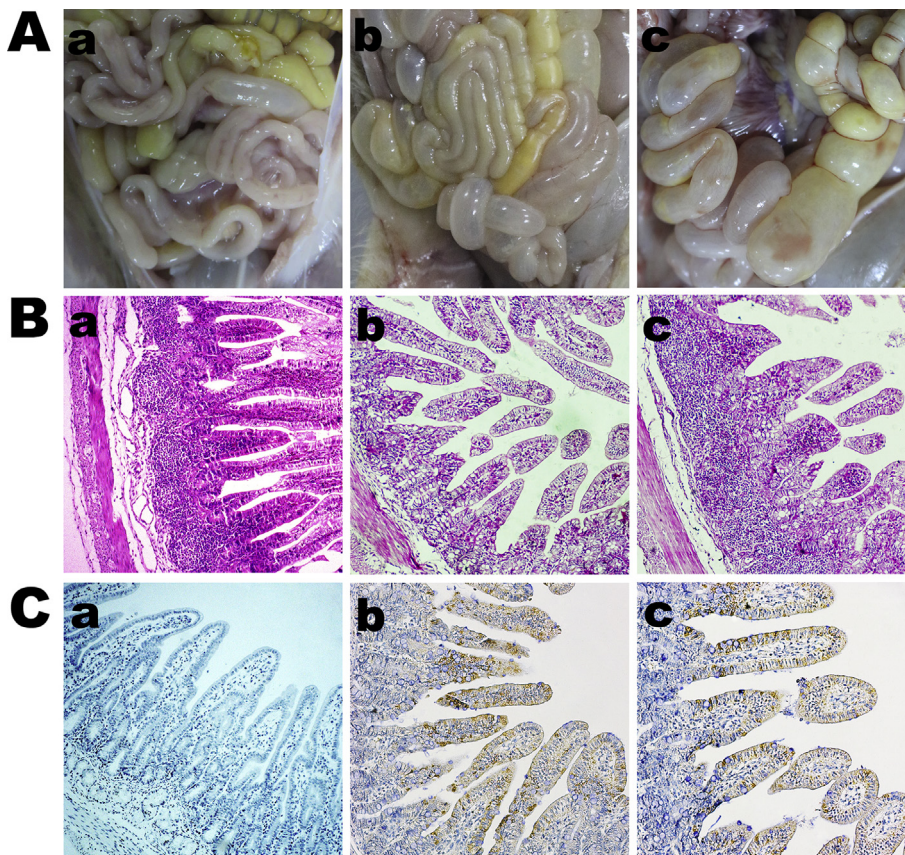


**Fig. 8.** Necropsy examinations, histopathology and immunohistochemical (IHC) of the intestines of piglet inoculated with PEDV HM2017 strain (P15) at 36 hpi. (A) Necropsy examinations of the intestines from HM2017-inoculated group and control group. (a) The control group showing no intestinal lesions. (b–c) The small intestines of HM2017-inoculated group showing distended, transparent, and filled with yellow fluid. (B) Hematoxylin and eosin-stained small intestinal sections from HM2017-inoculated group and control group (200× magnification). (a) The normal small intestinal villus was observed in control group. (b–c) The shortening, fusion, and sloughing of the small intestinal villus was observed in HM2017-inoculated group. (C) Detection of PEDV antigen by IHC analysis of small intestinal sections from HM2017-inoculated group and control group (200× magnification). (a) No PEDV antigen was detected in small intestines from control group. (b–c) PEDV antigen (brown color) was detected in small intestine epithelial cells from HM2017-inoculated group.



GII-b [5,33]. However, as a slight difference, 66.67% (12/18) of the experimental animals infected with strain HM2017 developed only mild diarrhea at 12 hpi, while strain HM2017 caused a significant increase in body temperature at 36 hpi with fecal shedding of high titers of viral RNA at 12 hpi and 100% mortality by 84 hpi [34]. Moreover, the viral loads were notably high in the duodenum, jejunum, ileum, cecum, and colon of the animals infected with strain HM2017, which is agreement with the report by Jung et al. (2014) [32]. Additionally, PEDV strain CH/JLDH/2016, which was classified into subgroup GII-a, was also highly pathogenic to piglets [18]. These data demonstrate that the PEDV strains of the developing GII-a subgroup are highly virulent and pose a serious threat to the pig populations in China.

*In vitro* cellular adaptability of PEDV is reported to significantly vary among different isolates [5,35,36]. Viral titers, representing viral proliferation *in vitro*, is an important indicator of PEDV candidate vaccine strains. Lin et al. (2017) reported that the highest titer of PEDV PC22A strain at passage 9 was  $6.00 \pm 0.67$  TCID<sub>50</sub>/mL, which is similar to that after 95 passages ( $5.50 \pm 0.84$  log<sub>10</sub>TCID<sub>50</sub>/mL), but significantly lower than after 100 ( $6.90 \pm 1.10$  log<sub>10</sub>TCID<sub>50</sub>/mL), 120 ( $6.9 \pm 0.74$  log<sub>10</sub>TCID<sub>50</sub>/mL), 140 ( $6.5 \pm 1.00$  log<sub>10</sub>TCID<sub>50</sub>/mL), and 160 ( $6.75 \pm 0.50$  log<sub>10</sub>TCID<sub>50</sub>/mL) passages [35]. Chen et al. (2019) reported that the infection titers of PEDV strain FJz1 at passages 5, 10, and 20 had peaked from  $5.44 \times 10^5$  to  $5.71 \times 10^5$  TCID<sub>50</sub>/mL [5]. Fan et al. (2017) reported that the infection titer of PEDV strain AH2012/12 at passages 10, 20, 30, 40, and 50 ranged from  $10^{4.5}$  to  $10^{6.5}$  TCID<sub>50</sub>/mL [33]. Yang et al. (2018) reported that the viral titers of PEDV strain QIAP1401 at passages 10, 40, and 70 were  $10^{6.5}$ ,  $10^{6.8}$ , and  $10^{7.0}$  TCID<sub>50</sub>/mL, respectively [36]. Shi et al. (2017) reported that the viral titer of the intestinal epithelial cell-adapted PEDV strain NJ reached  $10^{5.5}$  TCID<sub>50</sub>/mL at passage 45 [37]. Park et al. (2018) reported that the viral titer of PEDV strain PED-CUP-B2014 was  $10^6$  TCID<sub>50</sub>/mL at passage 40 [38]. Lee et al. (2015) reported that the infectious viral titers of PEDV strain KNU-141,112 during the first 30 passages ranged from  $10^{5.1}$  to  $10^{8.2}$  TCID<sub>50</sub>/mL [31]. In the present study, PEDV strain HM2017 exhibited good *in vitro* cellular adaptability. The infection titer of the 15th generation of viruses in Vero cells was  $1.33 \times 10^7$  TCID<sub>50</sub>/mL, which was greater than that of the control PEDV strain CV777. The infection titer of the 15th generation of PEDV strain HM2017 was similar to that of PEDV strain KNU-141,112, but higher than other previous reports to varying degrees. These data demonstrate that the GII-a subgroup PEDV strain HM2017 has potential as a vaccine candidate strain.

## 5. Conclusion

In conclusion, PEDV strain HM2017 was successfully isolated in China and clustered into the variant subgroup GII-a that are currently circulating in pig populations in China. PEDV strain HM2017 appeared to be highly virulent in suckling piglets, with disease characterized by severe clinical manifestations and intestinal lesions followed by relatively rapid death of the infected animals. PEDV strain HM2017 was well adapted to Vero cells, as evidenced by the rapid growth. Together, these data suggest that the prevalence of HM2017-like strains of the developing PEDV subgroup GII-a should be widely monitored in China and efficient vaccines should be developed based on these strains.

## Declaration of competing interest

The authors declare no conflict of interest.

## Acknowledgements

This work was supported by the National Key Research and Development Program of China (grant no. 2017YFD0501604-5), the National Natural Science Foundation of China (grant no. 31873011), the Outstanding Youth Science Foundation of Heilongjiang province

(grant no. JC2017007), the Heilongjiang Province Postdoctoral Science Foundation (grant no. LBH-Q16188), and Graduate innovative research projects in Heilongjiang Bayi Agricultural University (YJSCX2018-Z02/YJSCX2017-Z02).

## Appendix A. Supplementary data

Supplementary data to this article can be found online at <https://doi.org/10.1016/j.micpath.2019.103922>.

## References

- [1] M.B. Pensaert, P. de Bouck, A new coronavirus-like particle associated with diarrhea in swine, *Arch. Virol.* 58 (3) (1978) 243–247, <https://doi.org/10.1007/BF01317606>.
- [2] W. Li, H. Li, Y. Liu, Y. Pan, F. Deng, Y. Song, X. Tang, Q. He, New variants of porcine epidemic diarrhea virus, China, 2011, *Emerg. Infect. Dis.* 18 (8) (2012) 1350–1353, <https://doi.org/10.3201/eid1808.120002>.
- [3] J. Chen, X. Liu, D. Shi, H. Shi, X. Zhang, L. Feng, Complete genome sequence of a porcine epidemic diarrhea virus variant, *J. Virol.* 86 (6) (2012) 3408, <https://doi.org/10.1128/JVI.07150-11>.
- [4] D. Sun, X. Wang, S. Wei, J. Chen, L. Feng, Epidemiology and vaccine of porcine epidemic diarrhea virus in China: a mini-review, *J. Vet. Med. Sci.* 78 (3) (2016) 355–363, <https://doi.org/10.1292/jvms.15-0446>.
- [5] P. Chen, K. Wang, Y. Hou, H. Li, X. Li, L. Yu, Y. Jiang, F. Gao, W. Tong, H. Yu, Z. Yang, G. Tong, Y. Zhou, Genetic evolution analysis and pathogenicity assessment of porcine epidemic diarrhea virus strains circulating in part of China during 2011–2017, *Infect. Genet. Evol.* 69 (2019) 153–165, <https://doi.org/10.1016/j.meegid.2019.01.022>.
- [6] C.M. Lin, L.J. Saif, D. Marthaler, Q. Wang, Evolution, antigenicity and pathogenicity of global porcine epidemic diarrhea virus strains, *Virus Res.* 226 (2016) 20–39, <https://doi.org/10.1016/j.virusres.2016.05.023>.
- [7] S. Gallien, C. Fablet, L. Bigault, C. Bernard, O. Toulouse, M. Berri, Y. Blanchard, N. Rose, B. Grasland, Lessons learnt from a porcine epidemic diarrhea (PED) case in France in 2014: descriptive epidemiology and control measures implemented, *Vet. Microbiol.* 226 (2018) 9–14, <https://doi.org/10.1016/j.vetmic.2018.09.023>.
- [8] M.C. Niederwerder, R.A. Hesse, Swine enteric coronavirus disease: a review of 4 years with porcine epidemic diarrhoea virus and porcine deltacoronavirus in the United States and Canada, *Transboundary Emerg. Dis.* 65 (3) (2018) 660–675, <https://doi.org/10.1111/tbed.12823>.
- [9] Y. Sun, Y. Chen, X. Han, Z. Yu, Y. Wei, G. Zhang, Porcine epidemic diarrhea virus in Asia: an alarming threat to the global pig industry, *Infect. Genet. Evol.* 70 (2019) 24–26, <https://doi.org/10.1016/j.meegid.2019.02.013>.
- [10] L. Wang, B. Byrum, Y. Zhang, New variant of porcine epidemic diarrhea virus, United States, 2014, *Emerg. Infect. Dis.* 20 (5) (2014) 917–919, <https://doi.org/10.3201/eid2005.140195>.
- [11] R. Yamamoto, J. Soma, M. Nakanishi, R. Yamaguchi, S. Niinuma, Isolation and experimental inoculation of an S INDEL strain of porcine epidemic diarrhea virus in Japan, *Res. Vet. Sci.* 103 (2015) 103–106, <https://doi.org/10.1016/j.rvsc.2015.09.024>.
- [12] E. Wang, D. Guo, C. Li, S. Wei, Z. Wang, Q. Liu, B. Zhang, F. Kong, L. Feng, D. Sun, Molecular characterization of the ORF3 and S1 genes of porcine epidemic diarrhea virus non S-indelet strains in seven regions of China, 2015, *PLoS One* 11 (8) (2016) e0160561, <https://doi.org/10.1371/journal.pone.0160561>.
- [13] D. Hanke, A. Pohlmann, C. Sauter-Louis, D. Höper, J. Stadler, M. Ritzmann, A. Steinrigl, B.A. Schwarz, V. Akimkin, R. Fux, S. Blome, M. Beer, Porcine epidemic diarrhea in Europe: in-detail analyses of disease dynamics and molecular epidemiology, *Viruses* 9 (7) (2017) e177, <https://doi.org/10.3390/v9070177>.
- [14] J. Guo, L. Fang, X. Ye, J. Chen, S. Xu, X. Zhu, Y. Miao, D. Wang, S. Xiao, Evolutionary and genotypic analyses of global porcine epidemic diarrhea virus strains, *Transboundary Emerg. Dis.* 66 (1) (2019) 111–118, <https://doi.org/10.1111/tbed.12991>.
- [15] M.B. Boniotti, A. Papetti, A. Lavazza, G. Alborali, E. Sozzi, C. Chiapponi, S. Faccini, P. Bonilauri, P. Cordioli, D. Marthaler, Porcine epidemic diarrhea virus and discovery of a recombinant swine enteric coronavirus, Italy, *Emerg. Infect. Dis.* 22 (1) (2016) 83–87, <https://doi.org/10.3201/eid2201.150544>.
- [16] Q. Chen, P.C. Gauger, M.R. Stafne, J.T. Thomas, D.M. Madson, H. Huang, Y. Zheng, G. Li, J. Zhang, Pathogenesis comparison between the United States porcine epidemic diarrhoea virus prototype and S-INDEL-variant strains in conventional neonatal piglets, *J. Gen. Virol.* 97 (5) (2016) 1107–1121, <https://doi.org/10.1099/jgv.0.000419>.
- [17] X. Chen, X.X. Zhang, C. Li, H. Wang, H. Wang, X.Z. Meng, J. Ma, H.B. Ni, X. Zhang, Y. Qi, D. Sun, Epidemiology of porcine epidemic diarrhea virus among Chinese pig populations: a meta-analysis, *Microb. Pathog.* 129 (2019) 43–49, <https://doi.org/10.1016/j.micpath.2019.01.017>.
- [18] T. Zhu, S. Du, D. Cao, Z. Pei, Y. Guo, H. Shao, H. Wang, K. Wang, G. Hu, Isolation and identification of a variant subtype G 2b porcine epidemic diarrhea virus and S gene sequence characteristic, *Infect. Genet. Evol.* 71 (2019) 82–90, <https://doi.org/10.1016/j.meegid.2019.03.015>.
- [19] Y. Hou, C.M. Lin, M. Yokoyama, B.L. Yount, D. Marthaler, A.L. Douglas, S. Ghimire, Y. Qin, R.S. Baric, L.J. Saif, Q. Wang, Deletion of a 197-amino-acid region in the N-terminal domain of spike protein attenuates porcine epidemic diarrhea virus in

- piglets, *J. Virol.* 91 (14) (2017), <https://doi.org/10.1128/JVI.00227-17> e00227-17.
- [20] C.M. Lin, S. Ghimire, Y. Hou, P. Boley, S.N. Langel, A.N. Vlasova, L.J. Saif, Q. Wang, Pathogenicity and immunogenicity of attenuated porcine epidemic diarrhea virus PC22A strain in conventional weaned pigs, *BMC Vet. Res.* 15 (1) (2019) 26, <https://doi.org/10.1186/s12917-018-1756-x>.
- [21] S. Gallien, A. Moro, G. Lediguerher, V. Catinot, F. Paboef, L. Bigault, P.C. Gauger, N. Pozzi, M. Berri, E. Authié, N. Rose, B. Grasland, Limited shedding of an S-InDel strain of porcine epidemic diarrhea virus (PEDV) in semen and questions regarding the infectivity of the detected virus, *Vet. Microbiol.* 228 (2019) 20–25, <https://doi.org/10.1016/j.vetmic.2018.09.025>.
- [22] X. Liu, L. Zhang, Q. Zhang, P. Zhou, Y. Fang, D. Zhao, J. Feng, W. Li, Y. Zhang, Y. Wang, Evaluation and comparison of immunogenicity and cross-protective efficacy of two inactivated cell culture-derived GIIa- and GIIb-genotype porcine epidemic diarrhea virus vaccines in suckling piglets, *Vet. Microbiol.* 230 (2019) 278–282, <https://doi.org/10.1016/j.vetmic.2019.02.018>.
- [23] L. Zhang, X. Liu, Q. Zhang, P. Zhou, Y. Fang, Z. Dong, D. Zhao, W. Li, J. Feng, Y. Zhang, Y. Wang, Biological characterization and pathogenicity of a newly isolated Chinese highly virulent genotype GIIa porcine epidemic diarrhea virus strain, *Arch. Virol.* 164 (5) (2019) 1287–1295, <https://doi.org/10.1007/s00705-019-04167-3>.
- [24] N. Jiang, E. Wang, D. Guo, X. Wang, M. Su, F. Kong, D. Yuan, J. Zhai, D. Sun, Isolation and molecular characterization of parainfluenza virus 5 in diarrhea-affected piglets in China, *J. Vet. Med. Sci.* 80 (4) (2018) 590–593, <https://doi.org/10.1292/jvms.17-0581>.
- [25] L.J. Reed, H. Muench, A simple method for estimating fifty percent endpoints, *Am. J. Hyg.* 27 (1938) 493–497.
- [26] K. Tamura, G. Stecher, D. Peterson, A. Filipiński, S. Kumar, MEGA6: molecular evolutionary genetics analysis version 6.0, *Mol. Biol. Evol.* 30 (12) (2013) 2725–2729, <https://doi.org/10.1093/molbev/mst197>.
- [27] I. Letunic, P. Bork, Interactive Tree of Life (iTOL): an online tool for phylogenetic tree display and annotation, *Bioinformatics* 23 (1) (2007) 127–128, <https://doi.org/10.1093/bioinformatics/btl529>.
- [28] K.S. Lole, R.C. Bollinger, R.S. Paranjape, D. Gadkari, S.S. Kulkarni, N.G. Novak, R. Ingersoll, H.W. Sheppard, S.C. Ray, Full-length human immunodeficiency virus type 1 genomes from subtype C-infected seroconverters in India, with evidence of intersubtype recombination, *J. Virol.* 73 (1) (1999) 152–160.
- [29] D. Wang, X. Ge, D. Chen, J. Li, Y. Cai, J. Deng, L. Zhou, X. Guo, J. Han, H. Yang, The S gene is necessary but not sufficient for the virulence of porcine epidemic diarrhea virus novel variant strain BJ2011C, *J. Virol.* 92 (13) (2018) e00603–e00618, <https://doi.org/10.1128/JVI.00603-18>.
- [30] N. Dong, L. Fang, H. Yang, H. Liu, T. Du, P. Fang, D. Wang, H. Chen, S. Xiao, Isolation, genomic characterization, and pathogenicity of a Chinese porcine delta-coronavirus strain CHN-HN-2014, *Vet. Microbiol.* 196 (2016) 98–106, <https://doi.org/10.1016/j.vetmic.2016.10.022>.
- [31] S. Lee, Y. Kim, C. Lee, Isolation and characterization of a Korean porcine epidemic diarrhea virus strain KNU-141112, *Virus Res.* 208 (2015) 215–224, <https://doi.org/10.1016/j.virusres.2015.07.010>.
- [32] K. Jung, Q. Wang, K.A. Scheuer, Z. Lu, Y. Zhang, L.J. Saif, Pathology of US porcine epidemic diarrhea virus strain PC21A in gnotobiotic pigs, *Emerg. Infect. Dis.* 20 (4) (2014) 662–665, <https://doi.org/10.3201/eid2004.131685>.
- [33] B. Fan, Z. Yu, F. Pang, X. Xu, B. Zhang, R. Guo, K. He, B. Li, Characterization of a pathogenic full-length cDNA clone of a virulent porcine epidemic diarrhea virus strain AH2012/12 in China, *Virology* 500 (2017) 50–61, <https://doi.org/10.1016/j.virol.2016.10.011>.
- [34] Y. Wang, X. Gao, Y. Yao, Y. Zhang, C. Lv, Z. Sun, Y. Wang, X. Jia, J. Zhuang, Y. Xiao, X. Li, K. Tian, The dynamics of Chinese variant porcine epidemic diarrhea virus production in Vero cells and intestines of 2-day old piglets, *Virus Res.* 208 (2015) 82–88, <https://doi.org/10.1016/j.virusres.2015.06.009>.
- [35] C.M. Lin, Y. Hou, D.G. Marthaler, X. Gao, X. Liu, L. Zheng, L.J. Saif, Q. Wang, Attenuation of an original US porcine epidemic diarrhea virus strain PC22A via serial cell culture passage, *Vet. Microbiol.* 201 (2017) 62–71, <https://doi.org/10.1016/j.vetmic.2017.01.015>.
- [36] D.K. Yang, H.H. Kim, S.H. Lee, S.S. Yoon, J.W. Park, I.S. Cho, Isolation and characterization of a new porcine epidemic diarrhea virus variant that occurred in Korea in 2014, *J. Vet. Sci.* 19 (1) (2018) 71–78, <https://doi.org/10.4142/jvs.2018.19.1.71>.
- [37] W. Shi, S. Jia, H. Zhao, J. Yin, X. Wang, M. Yu, S. Ma, Y. Wu, Y. Chen, W. Fan, Y. Xu, Y. Li, Novel approach for isolation and identification of porcine epidemic diarrhea virus (PEDV) strain NJ using porcine intestinal epithelial cells, *Viruses* 9 (1) (2017) e19, <https://doi.org/10.3390/v9010019>.
- [38] J.E. Park, K.J. Kang, J.H. Ryu, J.Y. Park, H. Jang, D.J. Sung, J.G. Kang, H.J. Shin, Porcine epidemic diarrhea vaccine evaluation using a newly isolated strain from Korea, *Vet. Microbiol.* 221 (2018) 19–26, <https://doi.org/10.1016/j.vetmic.2018.05.012>.